

Gene Expression Profiles in Peripheral Lymphocytes by Arsenic Exposure and Skin Lesion Status in a Bangladeshi Population

Maria Argos,¹ Muhammad G. Kibriya,¹ Faruque Parvez,² Farzana Jasmine,¹ Muhammad Rakibuz-Zaman,⁴ and Habibul Ahsan^{1,3}

Departments of ¹Epidemiology and ²Environmental Health Sciences, Mailman School of Public Health, and ³Herbert Irving Comprehensive Cancer Center, Columbia University, New York, New York and ⁴Columbia University Arsenic Project in Bangladesh, Bangladesh

Abstract

Millions of individuals worldwide are chronically exposed to arsenic through their drinking water. In this study, the effect of arsenic exposure and arsenical skin lesion status on genome-wide gene expression patterns was evaluated using RNA from peripheral blood lymphocytes of individuals selected from the Health Effects of Arsenic Longitudinal Study. Affymetrix HG-U133A GeneChip (Affymetrix, Santa Clara, CA) arrays were used to measure the expression of ~22,000 transcripts. Our primary statistical analysis involved identifying differentially expressed genes between participants with and without arsenical skin lesions based on the significance analysis of microarrays statistic with an *a priori* defined 1% false discovery rate to minimize false positives. To better characterize differential expression, we also conducted Gene Ontology and pathway comparisons in addition to the gene-specific analyses. Four-

hundred sixty-eight genes were differentially expressed between these two groups, from which 312 differentially expressed genes were identified by restricting the analysis to female never-smokers. We also explored possible differential gene expression by arsenic exposure levels among individuals without manifest arsenical skin lesions; however, no differentially expressed genes could be identified from this comparison. Our findings show that microarray-based gene expression analysis is a powerful method to characterize the molecular profile of arsenic exposure and arsenic-induced diseases. Genes identified from this analysis may provide insights into the underlying processes of arsenic-induced disease and represent potential targets for chemoprevention studies to reduce arsenic-induced skin cancer in this population. (Cancer Epidemiol Biomarkers Prev 2006;15(7):1367–75)

Introduction

Arsenic contaminates the drinking water supply at a concentration greater than 50 µg/L for millions of people worldwide, with ~35 to 50 million of these individuals in Bangladesh (1, 2). Arsenic is a well-established human carcinogen (3); however, the exact mechanism by which it causes cancer has not been established. This is partly because there is no good animal model to study the toxicity of arsenic. Many of the human health effects of arsenic have been established based on epidemiologic studies, which have shown a significant association between the consumption of arsenic through drinking water and cancers of the skin, lung, bladder, liver, and kidney (4–8), neurologic disease (9), cardiovascular disease (10), and other nonmalignant diseases (11, 12). Premalignant skin lesions (melanosis, leucomelanosis, and keratosis) are an early manifestation and hallmark of arsenic toxicity and may indicate increased future risk of arsenic-related cancer (13). However, the molecular basis of arsenic-induced skin lesions and its progression to cancer is poorly understood.

Several microarray-based gene expression studies have been conducted to investigate the mechanism of arsenic toxicity (14–39). Only two of these studies were conducted in human populations (27, 35), whereas the rest were *in vitro* or animal studies. Lu et al. (27) examined aberrant gene expression

associated with arsenic-induced liver disease using cDNA microarrays that contained ~600 genes and found ~10% differentially expressed. The study used RNA that was extracted from liver biopsies of six exposed and six unexposed individuals. Wu et al. (35) examined differential gene expression associated with intermediate and high arsenic exposure (determined by blood arsenic concentration, 4.64–46.5 µg/L) compared with low arsenic exposure (blood arsenic concentration, 0–4.32 µg/L) using cDNA arrays that contained 708 known gene transcripts and found ~9% differentially expressed. RNA was extracted from peripheral blood lymphocytes of 24 participants. Both of these studies explored gene expression of a limited subset of genes, with <1,000 transcripts interrogated.

We conducted a microarray-based gene expression study among individuals chronically exposed to arsenic to assess whether arsenical skin lesion status and arsenic exposure level are associated with differential gene expression patterns. This study is the first, to our knowledge, to examine the effect of arsenic on genome-wide expression in humans. Through identifying differential patterns of expression, we hope to characterize the effect of arsenic and its outcomes, to better understand arsenic carcinogenesis, and to identify potential molecular targets for chemoprevention.

Materials and Methods

Study Population and Exposure Assessment. Forty individuals were selected from the Health Effects of Arsenic Longitudinal Study (HEALS) cohort for examination of gene expression profiles (40). The HEALS is an ongoing, population-based study examining both short-term and long-term health effects of arsenic exposure from drinking water in Bangladesh. In 2000, the study was launched in Araihasar,

Received 2/22/06; revised 5/3/06; accepted 5/17/06.

Grant support: NIH grants R01 CA102484, R01 CA107431, P42 ES10349, and P30 ES09089.

The costs of publication of this article were defrayed in part by the payment of page charges. This article must therefore be hereby marked advertisement in accordance with 18 U.S.C. Section 1734 solely to indicate this fact.

Requests for reprints: Habibul Ahsan, Department of Epidemiology, Mailman School of Public Health, Columbia University Medical Center, 722 West 168th Street, Room 720-G, New York, NY 10032. Phone: 212-305-7636; Fax: 212-342-2129. E-mail: habibul.ahsan@columbia.edu

Copyright © 2006 American Association for Cancer Research.

doi:10.1158/1055-9965.EPI-06-0106

Bangladesh, among a population of individuals chronically exposed to arsenic through groundwater consumption. The 40 individuals selected for this pilot study included 15 individuals with arsenical skin lesions and 25 individuals without such lesions. At the baseline interview of HEALS cohort participants, a clinical examination was conducted by study physicians to diagnose and identify skin lesions. Skin lesions included melanosis, leucomelanosis, and keratosis. Melanosis was characterized by the hyperpigmentation of the skin over wide body surface areas. Leucomelanosis was characterized by both hyperpigmentation and hypopigmentation of the skin over wide body surface areas. Keratosis was characterized by the general thickening of the skin of the palms and soles (41). The 25 individuals in this pilot study with no manifest arsenical skin lesions were sampled from the cohort by matching on gender and age (± 5 years) to the individuals with skin lesions.

A blood sample was collected from each participant at the time of recruitment into the parent HEALS cohort between October 2000 and May 2002; however, because these blood samples were not processed and stored in a manner suitable for isolating RNA, a separate blood sample was collected from each of these 40 individuals between February 2003 and March 2003, specifically for the examination of gene expression in this pilot study. Individual-level arsenic exposure was assessed based on urine samples collected as part of the parent HEALS follow-up between December 2002 and March 2004 and used to examine correlation with gene expression patterns in this study. Urinary total arsenic concentration was analyzed by graphite furnace atomic absorption spectrometry according to the method of Nixon et al. (42). Urinary creatinine was measured by a colorimetric Sigma Diagnostics kit (Sigma, St. Louis, MO), and urinary total arsenic concentration was subsequently expressed as micrograms per gram creatinine. Among the 40 participants, 28 subjects had both blood and urine samples used for this analysis collected within a 3-month period of each other (range, <1-11 months). From questionnaire data available at the time of urine sample collection, 28 participants (3 arsenical skin lesion cases and 25 nonlesion participants) indicated they drank from the same well as reported at enrollment into the parent cohort study and 6 arsenical skin lesion participants reported having switched their well before the time of both blood and urine sample collections used in these analyses. For these 34 individuals, the urine sample should reasonably reflect arsenic exposure at the time of blood collection. The remaining 6 arsenical skin lesion cases switched their well in the period of time between the blood and urine sample collections, for whom correlation between blood and urine samples may be problematic.

RNA was isolated from peripheral blood lymphocytes, processed, and analyzed for gene expression of each individual; the 40 samples were individually run requiring 40 microarrays. In these analyses, gene expression comparisons were only evaluated across arrays with a similar 3'/5' ratio for both *glyceraldehyde-3-phosphate dehydrogenase* and *β -actin* genes on the microarray. A 3'/5' ratio measure greater than 3 for these internal control genes indicates degraded RNA or incomplete *in vitro* transcription. Among the 40 microarrays, a single batch of 20 samples processed using the same *in vitro* transcription kit all had 3'/5' ratios greater than 3 for these internal control genes. All samples in the batch were from individuals with no manifest arsenical skin lesions and therefore were only used in analyses examining exposure level and not used in the comparison by skin lesion status. Among the 20 arrays run in the other *in vitro* transcription batch, all arrays had 3'/5' ratio measures less than 3 for the internal control genes; however, 4 arrays (samples from individuals with skin lesions) were excluded because they contained a background signal greater than 100. Arrays with average background signals greater than 100 were taken to

indicate a high level of nonspecific hybridization on those chips and excluded to preserve data quality. The remaining 16 arrays (11 skin lesion and 5 nonlesion samples) were comparable on other microarray quality metrics (43, 44), including noise (RawQ) <5, background signal <100, consistent scale factors, consistent detection of BioB and BioC spike controls, and consistent number of genes detected as present.

In subgroup exploratory analyses, subjects with no manifest arsenical skin lesions were subsequently categorized based on their creatinine-adjusted urinary total arsenic concentration. This study objective was explored separately in the two sets of nonlesion arrays ($n = 5$ and 20) to ensure the arrays were comparable in microarray quality variables as described previously. In one subgroup analysis ($n = 5$), 2 arrays were assigned low arsenic exposure based on a creatinine-adjusted urinary total arsenic concentration <70 $\mu\text{g/g}$ and 3 arrays assigned high arsenic exposure based on a creatinine-adjusted urinary total arsenic concentration >70 $\mu\text{g/g}$. This cut point was selected based on the distribution of creatinine-adjusted urinary total arsenic concentration in this nonlesion study sample ($n = 5$). The lowest urinary arsenic tertile (corresponding to the concentration range 48-67 $\mu\text{g/g}$) was categorized as low arsenic exposure. The highest two urinary arsenic tertiles (corresponding to the concentration range 90-215 $\mu\text{g/g}$) were categorized as high arsenic exposure. In the second subgroup analysis ($n = 20$) exploring this objective, 6 arrays were assigned low arsenic exposure based on a creatinine-adjusted urinary total arsenic concentration <162 $\mu\text{g/g}$ and 14 arrays assigned high arsenic exposure based on a creatinine-adjusted urinary total arsenic concentration >162 $\mu\text{g/g}$. This cut point was defined based on the distribution of creatinine-adjusted urinary total arsenic concentration in these nonlesion samples ($n = 20$). The lowest urinary arsenic tertile (corresponding to the concentration range 40-161 $\mu\text{g/g}$) was categorized as low arsenic exposure. The highest two urinary arsenic tertiles (corresponding to the concentration range 166-880 $\mu\text{g/g}$) were categorized as high arsenic exposure.

Blood Sample Processing. Whole venous blood samples were collected in 10 mL Vacutainer tubes containing 0.117 mL 15% (K3)EDTA and temporarily stored in a cooler box for transportation to the Dhaka laboratory. All blood samples were processed the day they were collected; processing took place within 2 to 8 hours after collection. Blood (8 mL) was transferred to a DNase- and RNase-free 15 mL tube and centrifuged at 2,400 rpm for 10 minutes at 25°C. Supernatant plasma was removed and preserved. Sterile 1 \times PBS stored at room temperature was added up to 15 mL and the blood was gently resuspended. The blood was then very slowly layered on approximately half-volume Ficoll-Paque (Amersham, Piscataway, NJ) and centrifuged at 2,700 rpm for 25 minutes. The opaque interphase layer, containing mononuclear cells, was transferred to another 15 mL DNase- and RNase-free tube and 1 \times PBS was added up to 15 mL. The tube was centrifuged at 1,000 rpm for 12 minutes and PBS was removed. Either 2 mL TRIzol reagent (Invitrogen, Carlsbad, CA) or 3.6 mL RLT buffer (Qiagen, Valencia, CA) was added to the mononuclear cells. After collection using syringe for homogenization, the mononuclear cells in TRIzol/RLT buffer were transferred to nonstick DNase- and RNase-free tubes for storage at -80°C. Within 2 to 3 months, the samples were transported on dry ice by air to the United States where they were stored at -80°C until RNA extraction.

RNA Extraction. RNA was extracted using the QIAamp RNA Blood Mini kit (Qiagen). The initial few steps were different for TRIzol and RLT preserved samples; however, the remainder was similar. TRIzol samples were incubated at 30°C for 5 minutes and chloroform (200 μL) was added per 1 mL TRIzol reagent. Samples were shaken vigorously by hand for 15 seconds and then incubated at 30°C for 3 minutes. The

samples were then centrifuged at 10,000 rpm for 15 minutes at 4°C. The aqueous phase containing RNA was carefully removed to a new RNase-free tube and 700 µL RLT was added per 200 µL aqueous phase and mixed well. Then, 500 µL molecular-grade absolute alcohol was added and mixed by pipetting. The sample was put on a QIAamp spin column sitting in a 2 mL collection tube. The rest of the procedure was conducted as per the Qiagen recommendation in the QIAamp RNA Blood Mini kit for RLT samples (described below). The RLT preserved samples were incubated at 37°C for 10 minutes. The remainder of the procedure was carried out at room temperature. For every 600 µL RLT sample, one QIAshredder column was used for centrifugation at 13,000 rpm for 2 minutes. The filter was discarded and 70% molecular grade alcohol (600 µL) was added per 600 µL filtered sample in RLT buffer and mixed well. The sample was then put on QIAamp spin column sitting in a 2 mL collection tube. The subsequent steps were similar for both TRIzol and RLT preserved samples. In short, the sample-filled QIAamp spin column was centrifuged and the filtrate was discarded. RNA was bound to the filter membrane. The membrane was washed with RW1 buffer, treated with DNase, and washed again with RW1 buffer followed by RPE buffer. RNA was eluted in RNase-free water.

Using a 1 µL sample, RNA quality and quantity were measured using the RNA 6000 Nano Chips in the Agilent 2100 Bioanalyzer (Palo Alto, CA). The A_{260}/A_{280} ratio was checked using 1 µL RNA on the ND-1000 spectrophotometer. All samples had A_{260}/A_{280} ratio > 1.9, indicating high-quality RNA. RNeasy MinElute Cleanup kit (Qiagen) was used to further concentrate the RNA. Integrity of RNA was checked again on the Agilent 2100 Bioanalyzer (an example is shown in Fig. 1). As seen in Fig. 1A, the two most distinct and intense peaks on the electropherogram correspond to the 18S and 28S rRNA. A 28S/18S ratio > 1.4 and the sum of both rRNA peak areas accounting for >33% of all RNA were taken as indicators of good-quality RNA.

Affymetrix GeneChip Standard Protocol. The Affymetrix (Santa Clara, CA) standard protocol has been described extensively elsewhere (45). Briefly, starting with 5 to 8 µg total RNA, we generated double-stranded cDNA using T7-(dT)₂₄ primer 5'-GGCCAGTGAATTGTAATACGACTCACTATAGG-GAGGCGG-(dT)₂₄-3' and SuperScript Choice System for cDNA synthesis (Invitrogen). The cDNA samples were purified using GeneChip Sample Cleanup Module (Affymetrix). Then, the *in vitro* transcription was done using the Enzo BioArray High-Yield RNA Transcription Labeling kit (Affymetrix) to produce biotin-labeled cRNA. Purification of cRNA was done using the GeneChip Sample Cleanup Module (Affymetrix). Quality and quantity of purified cRNA samples were checked by running a 1 µL sample on the ND-1000 spectrophotometer as well as on the Bioanalyzer. A A_{260}/A_{280} ratio between 1.9 and 2.2 was accepted. The adjusted cRNA yield was calculated as below:

$$\text{Adjusted cRNA yield} = \text{RNAm} - (\text{total RNAi})(y),$$

where RNAm is the amount of purified cRNA measured (µg), total RNAi is the starting amount of RNA (µg), and y is the fraction of cDNA used in the *in vitro* transcription reaction.

We fragmented 15 µg adjusted cRNA product using the 5× fragmentation buffer supplied in the GeneChip Sample Cleanup Module. Fragmented cRNA was run on the Bioanalyzer to ensure the fragmented size. Typical electropherograms of unfragmented and fragmented cRNA are shown in Fig. 1B and C, respectively. Biotin-labeled fragmented cRNA was then supplied to the core facility for hybridization onto the GeneChip HG-U133A array. After 16 to 18 hours of incubation, each microarray was washed, stained with streptavidin-phycoerythrin, and scanned by the high-resolution Affymetrix GeneChip

Scanner 3000 according to GeneChip Expression Analysis Technical Manual procedure (Affymetrix). After scanning, the raw intensities of each probe were stored in electronic files (.DAT and .CEL formats) by GCOS software (Affymetrix).

Statistical Analysis. The robust multiarray average method was applied to extract probe set signal intensities and to normalize all arrays (46). Before statistical analyses, genes were filtered by applying two exclusion criteria: (a) genes showing minimal variation (below the 80th percentile) across the set of arrays and (b) genes with >50% missing data were excluded from statistical analysis. Gene filtering was conducted separately for each distinct aim of the study and yielded separate lists of 4,456 genes each, which were used for the statistical analyses. Differentially expressed genes were identified using the significance analysis of microarrays statistic with a false discovery rate of 1% (47). The false discovery rate is the proportion of genes claimed to be differentially expressed that are false positives. Gene Ontology (GO) and pathway comparisons were also conducted based on the lists of 4,456 filtered genes using functional class scoring analysis as described by Pavlidis et al. (44). For each gene in a GO category, a *P* for differential expression comparing the two conditions of interest was computed. The set of *P*s for a GO category were summarized by two statistics: (a) the Fisher statistic *P* and (b) the Kolmogorov-Smirnov statistic *P*. A GO category was considered significantly differentially expressed if either significance level was <0.005. All GO categories with between 5 and 100 genes represented on the array were considered. Functional class scoring is a more powerful method of identifying differentially expressed gene classes than overrepresentation analysis or annotation of gene lists based on individually analyzed genes (44). Analysis of pathway comparisons were similar to the GO analysis; however, genes were grouped by KEGG or BioCarta pathways instead of GO categories (48). All analyses were done using BRB ArrayTools version 3.3.0 Beta 2 (49).

There is currently no predominate method to handle confounding variables in gene expression microarray studies. An effective technique for eliminating confounding in traditional epidemiologic studies is to match on potential confounding variables in the study design (50). For the current study, gender and age were considered potential confounders of gene expression in relation to arsenic exposure and skin lesion status. Their effects were considered *a priori* in the design stage of the study and matched on in the study participant selection. Additionally, analyses were restricted to never-smokers; smoking status was not included as a matching factor because there was no *a priori* reason to believe that this variable was a potential confounder because it is not an independent risk factor for arsenical skin lesions nor is it associated with arsenic exposure status.

Results

Gene expression profiles, using RNA derived from peripheral blood lymphocytes, were analyzed using Affymetrix HG-U133A GeneChip arrays. This microarray platform contains 22,283 probe sets for interrogation, including known genes and expressed sequence tags (51). To examine differential expression associated with arsenic-induced skin lesion status, the blood lymphocyte gene expression profiles of the subjects with no manifest skin lesions (*n* = 5) were compared with subjects with arsenical skin lesions (*n* = 11). The characteristics of the study participants are shown in Table 1. The mean (SD) well water arsenic concentration was 342.7 (258.1) µg/L for individuals with skin lesions and 39.6 (49.5) µg/L for individuals without skin lesions. The number of differentially expressed genes generated from the significance analysis of microarrays statistic was 468 (467 down-regulated and 1

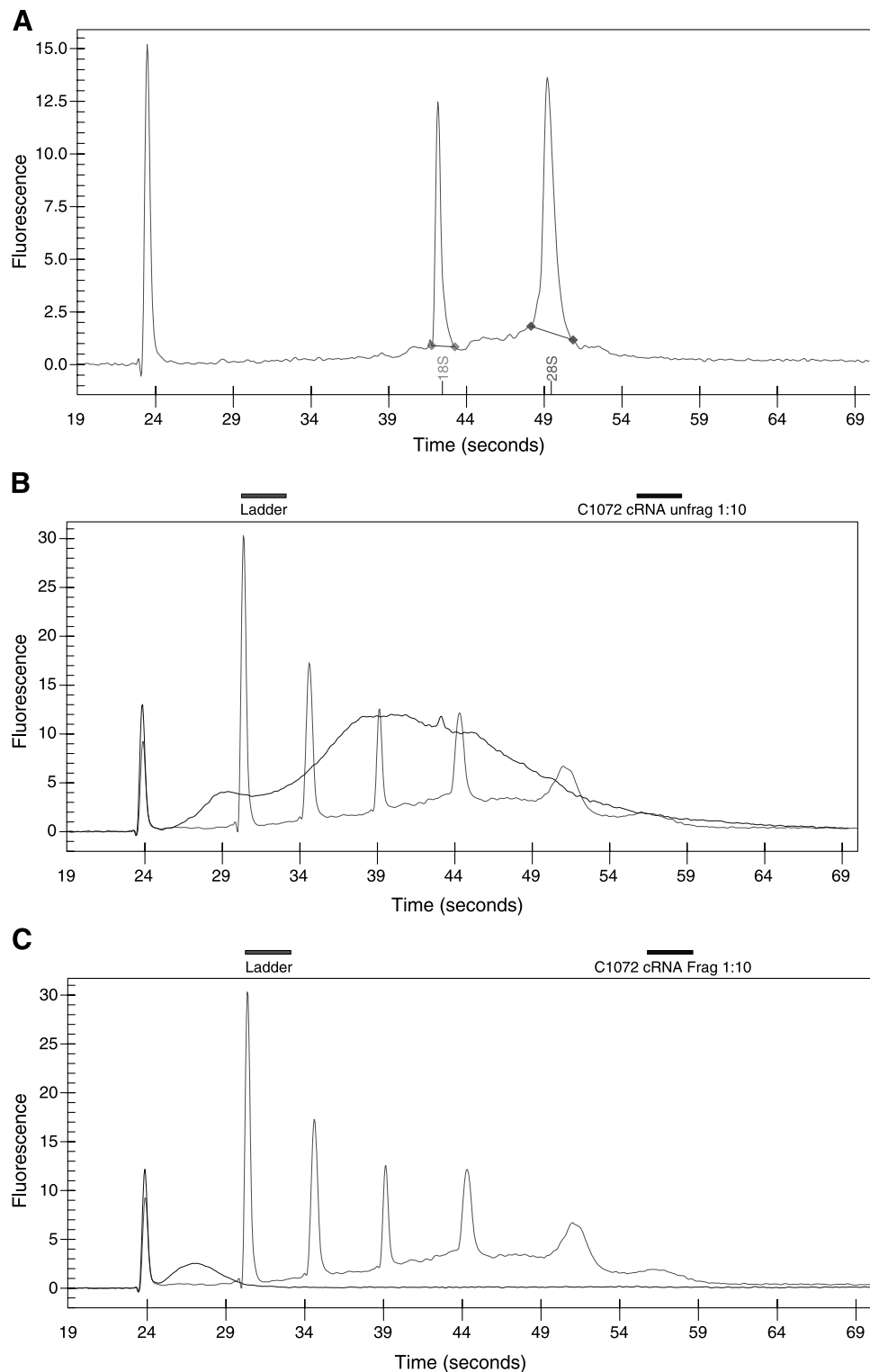


Figure 1. Electropherograms of RNA. **A.** Electropherogram shows two distinct peaks corresponding to 18S and 28S. The two peaks represent 16.69% and 28.25%, respectively, of the total area for RNA (collectively 44.94%) with a 28S/18S ratio of 1.69. **B.** In this electropherogram, the dark line represents purified 1:10 diluted unfragmented labeled cRNA superimposed with the ladder. After the initial spike, the ladder peaks correspond to 200, 500, 1,000, 2,000, and 4,000 bp, respectively. The unfragmented labeled cRNA ranges from 500 to 3,000 bp with the median lying between 1K and 2K. **C.** In this electropherogram, the dark line displays 1:10 diluted fragmented labeled cRNA superimposed with the ladder. The electropherogram shows effective fragmentation with the median ~60 to 70 bp.

up-regulated genes in the skin lesion group). Restricting the study sample to females only resulted in 330 differentially expressed genes (all down-regulated in the skin lesion group) between the skin lesion ($n = 9$) and nonlesion ($n = 5$) groups.

Further restricting the study sample to female never-smokers resulted in 312 differentially expressed genes (all down-regulated in the skin lesion group) between the skin lesion ($n = 8$) and nonlesion ($n = 5$) groups. The findings of the female

Table 1. Characteristics of study participants

	Skin lesions (<i>n</i> = 11)	No arsenical skin lesions* (<i>n</i> = 5)	No arsenical skin lesions* (<i>n</i> = 20)
Well water arsenic (µg/L), mean (SD)	342.7 (258.1)	39.6 (49.5)	94.5 (90.6)
Urinary total arsenic (µg/g), mean (SD)	467.8 (325.4)	109.8 (66.1)	279.7 (233.3)
Age (y), mean (SD)	35.0 (7.8)	38.0 (6.7)	26.4 (4.4)
Females, <i>n</i> (%)	9 (81.8)	5 (100.0)	14 (70.0)
Smokers, <i>n</i> (%)	2 (18.2)	0 (0.0)	3 (15.0)

*Two groups of nonlesion arrays were analyzed separately because they differed on microarray quality-control metrics.

never-smoker subgroup analysis are reported here, because we consider this gene list to have the least influence of gene expression variability due to extraneous factors. However, there was considerable overlap across the three gene lists generated; all 312 differentially expressed genes were present

in the gene list from the overall analysis and 310 were present in the gene list from the gender-restricted analysis. The top 50 down-regulated genes are listed in Table 2.

GO analysis, based on functional class scoring, revealed 41 significant GO categories, which are listed in Table 3. From the

Table 2. Genes differentially down-regulated in the skin lesion versus nonlesion comparison

Genbank accession no.	Gene symbol	Gene description	Ratio of geometric mean (lesion/nonlesion)
NM_002089	<i>CXCL2</i>	Chemokine (C-X-C motif) ligand 2	0.037
NM_004591	<i>CCL20</i>	Chemokine (C-C motif) ligand 20	0.059
NM_000576	<i>IL1B</i>	IL-1β	0.077
NM_019006	<i>ZA20D3</i>	Zinc finger, A20 domain containing 3	0.122
NM_000636	<i>SOD2</i>	Superoxide dismutase 2, mitochondrial	0.112
NM_000610	<i>CD44</i>	CD44 antigen (homing function and Indian blood group system)	0.112
NM_001001437	<i>CCL3</i>	Chemokine (C-C motif) ligand 3	0.091
NM_002852	<i>PTX3</i>	Pentraxin-related gene, rapidly induced by IL-1β	0.083
NM_000594	<i>TNF</i>	TNF (superfamily, member 2)	0.077
NM_000891	<i>KCNJ2</i>	Potassium inwardly rectifying channel, subfamily J, member 2	0.101
NM_003940	<i>USP13</i>	Ubiquitin-specific peptidase 13	0.158
NM_003965	<i>CCRL2</i>	Chemokine (C-C motif) receptor like 2	0.128
NM_003897	<i>IER3</i>	Immediate-early response 3	0.140
M10098	<i>SRP68</i>	Signal recognition particle 68 kDa	0.118
NM_004566	<i>PFKFB3</i>	6-Phosphofructo-2-kinase/fructose-2,6-biphosphatase 3	0.147
NM_014887	<i>PFAAP5</i>	Phosphonoformate immuno-associated protein 5	0.170
M27830	<i>SOX18</i>	Sex-determining region Y-box 18	0.152
NM_005346	<i>HSPA1B</i>	Heat shock protein 1B, 70-kDa	0.086
NM_007115	<i>TNFAIP6</i>	TNF-α-induced protein 6	0.115
NM_005066	<i>SFPQ</i>	Splicing factor proline/glutamine rich (polypyrimidine tract-binding protein associated)	0.189
NM_005751	<i>AKAP9</i>	A kinase (PRKA) anchor protein (yotiao) 9	0.198
NM_003414	<i>ZNF267</i>	Zinc finger protein 267	0.181
AL049987	<i>MGC22265</i>	Hypothetical protein MGC22265	0.210
NM_006186	<i>NR4A2</i>	Nuclear receptor subfamily 4, group A, member 2	0.170
NM_002919	<i>RFX3</i>	Regulatory factor X, 3 (influences HLA class II expression)	0.204
NM_001001723	<i>TMEM1</i>	Transmembrane protein 1	0.216
NM_004897	<i>MINPP1</i>	Multiple inositol polyphosphate histidine phosphatase, 1	0.228
NM_003143	<i>SSBP1</i>	ssDNA-binding protein 1	0.210
NM_018555	<i>ZNF331</i>	Zinc finger protein 331	0.199
NM_002922	<i>RG51</i>	Regulator of G-protein signaling 1	0.179
NM_002090	<i>CXCL3</i>	Chemokine (C-X-C motif) ligand 3	0.153
NM_002078	<i>GOLGA4</i>	Golgi autoantigen, golgin subfamily A, 4	0.234
NM_016166	<i>PIAS1</i>	Protein inhibitor of activated STAT 1	0.205
NM_014961	<i>RIPX</i>	Rap2-interacting protein X	0.238
NM_013293	<i>TRA2A</i>	Transformer 2α	0.221
NM_002984	<i>CCL4</i>	Chemokine (C-C motif) ligand 4	0.184
NM_000577	<i>IL1RN</i>	IL-1 receptor antagonist	0.174
NM_004233	<i>CD83</i>	CD83 antigen (activated B lymphocytes, immunoglobulin superfamily)	0.198
NM_020651	<i>PELL1</i>	Pellino homologue 1 (Drosophila)	0.245
NM_024116	<i>MGC5306</i>	Hypothetical protein MGC5306	0.242
NM_005414	<i>SKIL</i>	SKI-like	0.244
NM_002600	<i>PDE4B</i>	Phosphodiesterase 4B, cyclic AMP-specific (phosphodiesterase E4 dunce homologue, Drosophila)	0.242
NM_015675	<i>GADD45B</i>	Growth arrest and DNA damage-inducible, β	0.245
AU146791	<i>UBE2E1</i>	Ubiquitin-conjugating enzyme E2E 1 (UBC4/5 homologue, yeast)	0.268
NM_005004	<i>NDUFB8</i>	NADH dehydrogenase (ubiquinone) 1β subcomplex 8, 19 kDa	0.275
NM_002166	<i>ID2</i>	Inhibitor of DNA binding 2, dominant-negative helix-loop-helix protein	0.267
NM_015028	<i>TNIK</i>	TRAF2 and NCK-interacting kinase	0.264
NM_000575	<i>IL1A</i>	IL-1α	0.187
NM_000333	<i>ATXN7</i>	Ataxin 7	0.275
NM_003715	<i>VDP</i>	Vesicle docking protein p115	0.294

NOTE: Duplicate genes removed from the list.

Table 3. Gene Ontology categories from skin lesion and nonlesion comparison

GO Classification	No. genes	Fisher statistic permutation <i>P</i>	Kolmogorov-Smirnov permutation <i>P</i>
RNA splicing via transesterification reactions	54	0.00001	0.00050
RNA splicing via transesterification reactions with bulged adenosine as nucleophile	54	0.00001	0.00050
Nuclear mRNA splicing via spliceosome	54	0.00001	0.00050
RNA splicing	75	0.00001	0.00009
mRNA metabolism	88	0.00009	0.00001
Ubiquitin thioesterase activity	21	0.00010	0.00067
Ubiquitin-specific protease activity	21	0.00010	0.00067
Thioester hydrolase activity	21	0.00010	0.00067
mRNA processing	78	0.00010	0.00013
Ribonucleoprotein complex	89	0.00172	0.00009
tRNA modification	11	0.00196	0.03898
Translation	47	0.00300	0.08347
Ubiquitin-dependent protein catabolism	38	0.00309	0.00065
Modification-dependent protein catabolism	38	0.00309	0.00065
tRNA aminoacylation for protein translation	10	0.00316	0.07688
Amino acid activation	10	0.00316	0.07688
tRNA aminoacylation	10	0.00316	0.07688
RNA modification	16	0.00439	0.04396
Hexose transport	9	0.00656	0.00010
Monosaccharide transport	9	0.00656	0.00010
Glucose transport	9	0.00656	0.00010
P-P-bond hydrolysis-driven transporter activity	6	0.00816	0.00279
RNA localization	9	0.00917	0.00485
RNA-nucleus export	9	0.00917	0.00485
mRNA-nucleus export	9	0.00917	0.00485
Nucleic acid transport	9	0.00917	0.00485
RNA transport	9	0.00917	0.00485
mRNA transport	9	0.00917	0.00485
Establishment of RNA localization	9	0.00917	0.00485
Nucleolus	26	0.02319	0.00363
Protein amino acid glycosylation	22	0.02778	0.00144
Glycoprotein metabolism	25	0.03526	0.00422
Spliceosome complex	23	0.05039	0.00039
Protein folding	66	0.05608	0.00283
O-linked glycosylation	6	0.07142	0.00371
Carrier activity	45	0.08673	0.00482
Cyclic nucleotide phosphodiesterase activity	11	0.09273	0.00320
Glycerophosphoinositol inositolphosphodiesterase activity	11	0.09273	0.00320
Ubiquitin ligase complex	83	0.09814	0.00134
Phosphoric diester hydrolase activity	13	0.14050	0.00118
Unfolded protein binding	31	0.15627	0.00389

pathway comparison, one significant pathway was identified that could discriminate between the skin lesion ($n = 11$) and the nonlesion ($n = 5$) classes (Table 4). Additional analyses within the skin lesion group only ($n = 11$) to assess the influence of arsenic exposure based on well water and urinary

arsenic concentrations did not reveal any differentially expressed genes. Analyses by skin lesion severity also did not reveal any differentially expressed genes.

To explore differentially expressed genes associated with arsenic exposure, the gene expression profiles from blood

Table 4. Pathway comparison from skin lesion and nonlesion comparison restricted to female never-smokers

Pathway	No. genes	Fisher statistic permutation <i>P</i>	Kolmogorov-Smirnov permutation <i>P</i>
Signal transduction through IL-1 receptor	12	0.00396	0.02551
Genbank accession no.	Gene symbol	Gene description	
NM_002228	<i>JUN</i>	v-jun sarcoma virus 17 oncogene homologue (avian)	
NM_020529	<i>NFKBIA</i>	Nuclear factor of κ light polypeptide gene enhancer in B-cell inhibitor, α	
NM_001315	<i>MAPK14</i>	Mitogen-activated protein kinase 14	
NM_000576	<i>IL1B</i>	IL-1 β	
NM_000600	<i>IL6</i>	IL-6 (IFN- β 2)	
NM_004620	<i>TRAF6</i>	TNF receptor-associated factor 6	
NM_000594	<i>TNF</i>	TNF (superfamily, member 2)	
NM_000575	<i>IL1A</i>	IL-1 α	
NM_003998	<i>NFKB1</i>	Nuclear factor of κ light polypeptide gene enhancer in B cells 1 (p105)	
NM_001278	<i>CHUK</i>	Conserved helix-loop-helix ubiquitous kinase	
NM_003188	<i>MAP3K7</i>	Mitogen-activated protein kinase kinase kinase 7	
XM_042066	<i>MAP3K1</i>	Mitogen-activated protein kinase kinase kinase 1	

lymphocytes of individuals with low arsenic exposure were compared with those from individuals with high arsenic exposure, indicated by creatinine-adjusted urinary total arsenic concentration. Arsenic exposure was defined by tertile of creatinine-adjusted urinary total arsenic concentration for the arrays. These analyses were conducted separately for the two nonlesion sample populations, with arrays restricted to *in vitro* transcription batch ($n = 5$ and 20) to ensure comparability in microarray quality variables. The low and high arsenic exposure groups were similar in age, gender, and smoking status (data not shown). Within the 5-array nonlesion sample, the mean (SD) creatinine-adjusted urinary total arsenic concentration was 144.7 (63.9) $\mu\text{g/g}$ for the high arsenic exposure group and 57.5 (13.4) $\mu\text{g/g}$ for the low arsenic exposure group. Within the 20-array nonlesion sample, the mean (SD) creatinine-adjusted urinary total arsenic concentration was 346.6 (250.5) $\mu\text{g/g}$ for the high arsenic exposure group and 123.5 (44.2) $\mu\text{g/g}$ for the low arsenic exposure group. Statistical analysis did not reveal any differentially expressed genes by urinary arsenic exposure status in either sample population. Recategorization and analysis by well water arsenic concentration status in both sample populations yielded no differentially expressed genes.

Discussion

To our knowledge, this is the first molecular epidemiologic study to explore alterations in genome-wide expression due to arsenic exposure and arsenic-induced toxicity in a currently exposed human population. Only two prior *in vivo* studies had been conducted, which explored a subset of genes differentially expressed in relation to arsenic exposure or arsenic-induced disease (27, 35). Using the Affymetrix HG-U133A GeneChip, we have identified differentially expressed genes in peripheral blood lymphocytes of arsenic-exposed individuals and individuals with arsenical skin lesions.

In the present study, the effect of arsenic exposure was assessed among a population of individuals who have been chronically exposed to arsenic through groundwater consumption and were currently exposed at the time of blood sample collection for this pilot study. The HEALS cohort provided the sampling frame to examine individuals exposed to arsenic with no clinical evidence of premalignant skin lesions compared with individuals with manifest arsenical skin lesions. Thus, the effect of both arsenic exposure and exposure-related disease process could be examined. Study participants were matched on age and gender to minimize variability in gene expression that may be due to these confounding factors. Despite the restriction of samples in these analyses to *in vitro* transcription batch, the comparison groups still remained comparable on gender and age. Furthermore, the samples were collected from a population of individuals who are relatively homogenous in ethnicity and dietary intake, which again served to minimize variability due to extraneous factors. Although smoking status was not included as a matching factor, the effect of smoking was removed by restricting analyses to never-smokers.

In this study, we evaluated the joint effect of arsenic exposure and arsenical skin lesion status on gene expression. GO categories found to be differentially expressed between individuals with arsenical skin lesions compared with exposed individuals without such lesions broadly included RNA metabolism, hydrolase activity, ribonucleoprotein complex, translation, cellular protein catabolism, amino acid activation, transport and transporter activity, and glycoprotein metabolism. Additionally, signal transduction through the interleukin (IL)-1 receptor was identified as a significant pathway of differentially expressed genes between the arsenical skin lesion and nonlesion groups. Research has shown that this pathway

plays an important role in skin (52, 53), including the skin repair process (54). The IL-1 receptor pathway may lead to the activation of nuclear factor- κ B and p38 pathways (54); thus, the down-regulation of which may be indicative of deficiency in wound healing among the arsenical skin lesion cases.

Most genes differentially expressed in analyses between arsenical skin lesion cases and noncases were down-regulated. However, in the analysis between arsenical skin lesion cases ($n = 11$) and noncases ($n = 5$), we found 3.3-fold up-regulation of *thymopoietin*, a gene that has been implicated in the initiation of DNA replication (55). Furthermore, an *in vitro* study found that *thymopoietin* was overexpressed in cancer cell lines (56).

We have identified several genes that have been implicated in carcinogenesis. The *superoxide dismutase 2* gene, located at chromosomal region 6q25.3, encodes a free radical-scavenging enzyme that is the first line of defense against oxidative stress. Arsenic has been implicated as a source of reactive oxygen species (57-59). Additionally, polymorphisms in this gene have been associated with cancer (60). Some evidence from *in vitro* studies suggests that *superoxide dismutase 2* may act as a tumor suppression gene (61-65), with increased expression of *superoxide dismutase 2* having been shown to suppress the cancer phenotype in a large number of mammalian tumor cells, including human melanoma cells (61, 62). We observed down-regulated expression of *superoxide dismutase 2* in individuals with skin lesions, which may indicate an increased vulnerability to reactive oxygen species generated by arsenic in individuals with manifest arsenic toxicity. A second gene of interest is *tumor necrosis factor (TNF)* that is located at chromosomal region 6p21.3. This gene encodes a cytokine that is involved in cell proliferation, differentiation, apoptosis, lipid metabolism, and coagulation. Furthermore, studies have shown arsenic to be an inducer of TNF (66, 67). TNF is thought to trigger a chemokine signal response, including chemokine factor CCL20 (68). In this study, we have observed down-regulated TNF expression among individuals with arsenical skin lesions and down-regulated expression of CCL20, providing credence to the suppression of a chemokine response pathway in arsenic toxicity. There is evidence to indicate that TNF is released early in response to skin wounds or inflammation (69), which may suggest that the down-regulated expression of TNF observed in arsenical skin lesion cases is also indicative of deficient wound healing.

In future analyses, we plan to examine the correspondence of the current study findings using peripheral blood lymphocytes to a study examining gene expression from the target tissue of interest (e.g., skin lesion tissues). It is currently not well known whether gene expression in blood lymphocytes is a valid proxy for gene expression in the target tissue of interest and needs to be explored in future research.

A limitation of the present study was the extent of incomplete *in vitro* transcription among the nonlesion samples, which limited our ability to explore differential gene expression by arsenic exposure status only. After RNA extraction, sample quantity and quality was assessed, which indicated good RNA quality for all samples; therefore, the poor 3'/5' ratio in the *glyceraldehyde-3-phosphate dehydrogenase* and β -*actin* genes are indicative of incomplete *in vitro* transcription occurring in an entire batch as opposed to sample degradation in this study. The current analysis was limited to separate comparisons of 5 and 20 samples from individuals with relatively varied arsenic exposure. The lack of differentially expressed genes from these comparisons was most likely due to small sample size and heterogeneous exposure categories as opposed to the absence of a biological effect by arsenic on gene expression. In future studies, we hope to evaluate the effect of arsenic exposure in a dose-dependent manner on gene expression.

Although the Affymetrix HG-U133A GeneChip array measured genome-wide expression, the use of this platform

assessed mRNA from coding regions of the genome only. Recent evidence has suggested the importance of RNA from noncoding regions that may play key roles in carcinogenesis and other processes (70-72). A limitation of the current microarray technology used in this experiment (or any other experiments using generic reverse transcription-PCR) is that only RNA with a polyadenylic acid tail is amplified and reverse transcribed. A recent study reported that a substantial proportion of transcribed messages in the genome may include RNA without polyadenylic acid tail (73) and thus may not be detected in the currently available microarray-based gene expression analyses.

In conclusion, our findings show that microarray-based gene expression analysis is a powerful method to characterize the molecular profile of arsenic exposure and arsenic-induced diseases. Genes identified from this analysis may provide insights into the underlying disease mechanisms of arsenic and represent targets for disease prevention.

References

- Chowdhury A. Arsenic crisis in Bangladesh. *Sci Am* 2004;291:86-91.
- British Geological Survey. Groundwater studies for arsenic contamination in Bangladesh—phase 1 findings; 1999 [cited 2005 Apr 14]. Available from: <http://www.bgs.ac.uk/arsenic/>.
- IARC. IARC monographs on the evaluation of the carcinogenic risks to humans: arsenic and arsenic compounds (group 1). Lyon: IARC; 1987.
- Chen CJ, Chen CW, Wu MM, Kou TL. Cancer potential in liver, lung, bladder and kidney due to ingested inorganic arsenic in drinking water. *Br J Cancer* 1992;66:888-92.
- Hopenhayn-Rich C, Biggs ML, Fuchs A, et al. Bladder cancer mortality associated with arsenic in drinking water in Argentina. *Epidemiology* 1996;7:117-24.
- Hopenhayn-Rich C, Biggs ML, Smith AH. Lung and kidney cancer mortality associated with arsenic in drinking water in Cordoba, Argentina. *Int J Epidemiol* 1998;27:561-9.
- Smith AH, Goycolea M, Haque R, Biggs ML. Marked increase in bladder and lung cancer mortality in a region of northern Chile due to arsenic in drinking water. *Am J Epidemiol* 1998;147:660-9.
- Tseng WP. Effects and dose-response relationships of skin cancer and blackfoot disease with arsenic. *Environ Health Perspect* 1977;19:109-19.
- Brouwer OF, Onkenhout W, Edelbroek PM, de Kom JF, de Wolff FA, Peters AC. Increased neurotoxicity of arsenic in methylenetetrahydrofolate reductase deficiency. *Clin Neurol Neurosurg* 1992;94:307-10.
- Wu M, Kuo TL, Hwang YH, Chen CJ. Dose-response relation between arsenic concentration in well water and mortality from cancers and vascular diseases. *Am J Epidemiol* 1989;130:1123-32.
- Rahman M, Tondel M, Ahmad SA, Axelson O. Diabetes mellitus associated with arsenic exposure in Bangladesh. *Am J Epidemiol* 1988;148:198-203.
- Rahman M, Tondel M, Ahmad SA, Chowdhury IA, Faruquee MH, Axelson O. Hypertension and arsenic exposure in Bangladesh. *Hypertension* 1999;33:74-8.
- National Research Council. Arsenic in drinking water 2001 update. Washington (DC): National Academy Press; 2001.
- Ahn WS, Bae SM, Lee KH, et al. Comparison of effects of As₂O₃ and As₄O₆ on cell growth inhibition and gene expression profiles by cDNA microarray analysis in SiHa cells. *Oncol Rep* 2004;12:573-80.
- Bae DS, Hanneman WH, Yang RS, Campaign JA. Characterization of gene expression changes associated with MNNG, arsenic, or metal mixture treatment in human keratinocytes: application of cDNA microarray technology. *Environ Health Perspect* 2002;110:931-41.
- Bae DS, Handa RJ, Yang RS, Campaign JA. Gene expression patterns as potential molecular biomarkers for malignant transformation in human keratinocytes treated with MNNG, arsenic, or a metal mixture. *Toxicol Sci* 2003;74:32-42.
- Chen H, Li S, Liu J, Diwan BA, Barrett JC, Waalkes MP. Chronic inorganic arsenic exposure induces hepatic global and individual gene hypomethylation: implications for arsenic hepatocarcinogenesis. *Carcinogenesis* 2004;25:1779-86.
- Chen H, Liu J, Merrick BA, Waalkes MP. Genetic events associated with arsenic-induced malignant transformation: applications of cDNA microarray technology. *Mol Carcinog* 2001;30:79-87.
- Chen H, Liu J, Zhao CQ, Diwan BA, Merrick BA, Waalkes MP. Association of c-myc overexpression and hyperproliferation with arsenite-induced malignant transformation. *Toxicol Appl Pharmacol* 2001;175:260-8.
- Chou WC, Chen HY, Yu SL, Cheng L, Yang PC, Dang CV. Arsenic suppresses gene expression in promyelocytic leukemia cells partly through Sp1 oxidation. *Blood* 2005;106:304-10.
- Dvorakova K, Payne CM, Tome ME, et al. Molecular and cellular characterization of imexon-resistant RPMI8226/1 myeloma cells. *Mol Cancer Ther* 2002;1:185-95.
- Hamadeh HK, Trouba KJ, Amin RP, Afshari CA, Germolec D. Coordination of altered DNA repair and damage pathways in arsenite-exposed keratinocytes. *Toxicol Sci* 2002;69:306-16.
- Hirano S, Cui X, Li S, et al. Difference in uptake and toxicity of trivalent and pentavalent inorganic arsenic in rat heart microvessel endothelial cells. *Arch Toxicol* 2003;77:305-12.
- Kanzawa T, Zhang L, Xiao L, Germano IM, Kondo Y, Kondo S. Arsenic trioxide induces autophagic cell death in malignant glioma cells by upregulation of mitochondrial cell death protein BNIP3. *Oncogene* 2005;24:980-91.
- Liu J, Chen H, Miller DS, et al. Overexpression of glutathione S-transferase II and multidrug resistance transport proteins is associated with acquired tolerance to inorganic arsenic. *Mol Pharmacol* 2001;60:302-9.
- Liu J, Xie Y, Ward JM, Diwan BA, Waalkes MP. Toxicogenomic analysis of aberrant gene expression in liver tumors and nontumorous livers of adult mice exposed *in utero* to inorganic arsenic. *Toxicol Sci* 2004;77:249-57.
- Lu T, Liu J, LeCluyse EL, Zhou YS, Cheng ML, Waalkes MP. Application of cDNA microarray to the study of arsenic-induced liver diseases in the population of Guizhou, China. *Toxicol Sci* 2001;59:185-92.
- Nasr R, Rosenwald A, El-Sabban ME, et al. Arsenic/interferon specifically reverses 2 distinct gene networks critical for the survival of HTLV-1-infected leukemic cells. *Blood* 2003;101:4576-82.
- Rea MA, Gregg JP, Qin Q, Phillips MA, Rice RH. Global alteration of gene expression in human keratinocytes by inorganic arsenic. *Carcinogenesis* 2003;24:747-56.
- Wang HY, Liu SX, Zhang M. Gene expression profile changes in NB4 cells induced by arsenic trioxide. *Acta Pharmacol Sin* 2003;24:646-50.
- Wang H, Liu S, Lu X, Zhao X, Chen S, Li X. Gene expression profile changes in NB4 cells induced by realgar. *Chin Med J (Engl)* 2003;116:1074-7.
- Waring JF, Jolly RA, Ciurlionis R, et al. Clustering of hepatotoxins based on mechanism of toxicity using gene expression profiles. *Toxicol Appl Pharmacol* 2001;175:28-42.
- Waring JF, Ciurlionis R, Jolly RA, Heindel M, Ulrich RG. Microarray analysis of hepatotoxins *in vitro* reveals a correlation between gene expression profiles and mechanisms of toxicity. *Toxicol Lett* 2001;120:359-68.
- Wei M, Arnold L, Cano M, Cohen SM. Effects of co-administration of antioxidants and arsenicals on the rat urinary bladder epithelium. *Toxicol Sci* 2005;83:237-45.
- Wu M, Chiou HY, Ho IC, Chen CJ, Lee TC. Gene expression of inflammatory molecules in circulating lymphocytes from arsenic-exposed human subjects. *Environ Health Perspect* 2003;111:1429-38.
- Xie D, Yin S, Ou Y, et al. Arsenic trioxide (As₂O₃) induced apoptosis and its mechanisms in a human esophageal squamous carcinoma cell line. *Chin Med J (Engl)* 2002;115:280-5.
- Xie Y, Trouba KJ, Liu J, Waalkes MP, Germolec DR. Biokinetics and subchronic toxic effects of oral arsenite, arsenate, monomethylarsonic acid, and dimethylarsinic acid in v-Ha-ras transgenic (Tg.AC) mice. *Environ Health Perspect* 2004;112:1255-63.
- Yih LH, Peck K, Lee TC. Changes in gene expression profiles of human fibroblasts in response to sodium arsenite treatment. *Carcinogenesis* 2002;23:867-76.
- Zheng XH, Watts GS, Vaught S, Gandolfi AJ. Low-level arsenite induced gene expression in HEK293 cells. *Toxicology* 2003;187:39-48.
- Ahsan H, Chen Y, Parvez F, et al. Health Effects of Arsenic Longitudinal Study (HEALS): description of a multidisciplinary epidemiologic investigation. *J Expo Sci Environ Epidemiol* 2006;16:191-205.
- Alain G, Tousignant J, Rozenfarb E. Chronic arsenic toxicity. *Int J Dermatol* 1993;32:899-901.
- Nixon DE, Mussmann GV, Eckdahl SJ, Moyer TP. Total arsenic in urine: palladium-persulfate vs nickel as a matrix modifier for graphite furnace atomic absorption spectrophotometry. *Clin Chem* 1991;37:1575-9.
- Finkelstein DB. Trends in the quality of data from 5168 oligonucleotide microarrays from a single facility. *J Biomol Tech* 2005;16:143-53.
- Pavlidis P, Qin J, Arango V, Mann JJ, Sibille E. Using the gene ontology for microarray data mining: a comparison of methods and application to age effects in human prefrontal cortex. *Neurochem Res* 2004;29:1213-22.
- Affymetrix, Inc. GeneChip: expression analysis technical manual. Santa Clara (CA): Affymetrix; 2001.
- Irizarry RA, Bolstad BM, Collin F, Cope LM, Hobbs B, Speed TP. Summaries of Affymetrix GeneChip probe level data. *Nucleic Acids Res* 2003;31:e15.
- Tusher V, Tibshirani R, Chu G. Significance analysis of microarrays applied to the ionizing radiation response. *Proc Natl Acad Sci U S A* 2001;98:5116-21.
- Simon R, Lam A. BRB ArrayTools User Guide, version 3.3. Biometric Research Branch, National Cancer Institute; 2005 [cited 2005 Jul 28]. Available from: <http://Linus.nci.nih.gov/brb/>.
- Simon R, Lam A. BRB ArrayTools, version 3.3.0 Beta_2; 2005 [cited 2005 Jun 13]. Available from: <http://Linus.nci.nih.gov/BRB-ArrayTools.html>.
- Rothman K, Greenland S. Modern epidemiology. 2nd ed. New York: Lippincott, Williams & Wilkins; 1998.
- Affymetrix Inc. GeneChip human genome arrays: data sheet; 2003-04 [cited 2005 Jul 23]. Available from: http://www.affymetrix.com/support/technical/datasheets/human_datashet.pdf.
- Dower SK, Qvarnstrom EE, Page RC, et al. Biology of the interleukin-1 receptor. *J Invest Dermatol* 1990;94:68-73S.
- Labow M, Shuster D, Zetterstrom M, et al. Absence of IL-1 signaling and reduced inflammatory response in IL-1 type I receptor-deficient mice. *J Immunol* 1997;159:2452-61.

54. Takami Y, Motoki T, Yamamoto I, Gohda E. Synergistic induction of hepatocyte growth factor in human skin fibroblasts by the inflammatory cytokines interleukin-1 and interferon- γ . *Biochem Biophys Res Commun* 2005;327:212–7.
55. Martins S, Eikvar S, Furukawa K, Collas P. HA95 and LAP2 β mediate a novel chromatin-nuclear envelope interaction implicated in initiation of DNA replication. *J Cell Biol* 2003;160:177–88.
56. Weber PJ, Eckhard CP, Gonser S, Otto H, Folkers G, Beck-Sickingler AG. On the role of thymopoietins in cell proliferation. Immunochemical evidence for new members of the human thymopoietin family. *Biol Chem* 1999;380:653–60.
57. Hei TK, Liu SX, Waldren C. Mutagenicity of arsenic in mammalian cells: role of reactive oxygen species. *Proc Natl Acad Sci U S A* 1998;95:8103–7.
58. Kessel M, Liu SX, Xu A, Santella R, Hei TK. Arsenic induces oxidative DNA damage in mammalian cells. *Mol Cell Biochem* 2002;234–235:301–8.
59. Liu SX, Athar M, Lippai I, Waldren C, Hei TK. Induction of oxyradicals by arsenic: implication for mechanism of genotoxicity. *Proc Natl Acad Sci U S A* 2001;98:1643–8.
60. Hung RJ, Boffetta P, Brennan P, et al. Genetic polymorphisms of MPO, COMT, MnSOD, NQO1, interactions with environmental exposures and bladder cancer risk. *Carcinogenesis* 2004;25:973–8.
61. Bravard A, Cherbonnel-Lasserre C, Reillaudou M, Beaumatin J, Dutrillaux B, Luccioni C. Modifications of the antioxidant enzymes in relation to chromosome imbalances in human melanoma cell lines. *Melanoma Res* 1998;8:329–35.
62. Church SL, Grant JW, Ridnour LA, et al. Increased manganese superoxide dismutase expression suppresses the malignant phenotype of human melanoma cells. *Proc Natl Acad Sci U S A* 1993;90:3113–7.
63. Liu R, Oberley TD, Oberley LW. Transfection and expression of MnSOD cDNA decreases tumor malignancy of human oral squamous carcinoma SCC-25 cells. *Hum Gene Ther* 1997;8:585–95.
64. Ough M, Lewis A, Zhang Y, et al. Inhibition of cell growth by over-expression of manganese superoxide dismutase (MnSOD) in human pancreatic carcinoma. *Free Radic Res* 2004;38:1223–33.
65. Venkataraman S, Jiang X, Weydert C, et al. Manganese superoxide dismutase overexpression inhibits the growth of androgen-independent prostate cancer cells. *Oncogene* 2005;24:77–89.
66. Das S, Santra A, Lahiri S, Guha Mazumder DN. Implications of oxidative stress and hepatic cytokine (TNF- α and IL-6) response in the pathogenesis of hepatic collagenesis in chronic arsenic toxicity. *Toxicol Appl Pharmacol* 2005;204:18–26.
67. Germolec DR, Spalding J, Boorman GA, et al. Arsenic can mediate skin neoplasia by chronic stimulation of keratinocyte-derived growth factors. *Mutat Res* 1997;386:209–18.
68. Spiekstra SW, Toebak MJ, Sampat-Sardjoepersad S, et al. Induction of cytokine (interleukin-1 α and tumor necrosis factor- α) and chemokine (CCL20, CCL27, and CXCL8) alarm signals after allergen and irritant exposure. *Exp Dermatol* 2005;14:109–16.
69. Bacci S, Romagnoli P, Norelli GA, Forestieri AL, Bonelli A. Early increase in TNF- α -containing mast cells in skin lesions. *Int J Legal Med* 2006;120:138–42.
70. Chan JA, Krichevsky AM, Kosik KS. MicroRNA-21 is an antiapoptotic factor in human glioblastoma cells. *Cancer Res* 2005;65:6029–33.
71. Esau C, Kang X, Peralta E, et al. MicroRNA-143 regulates adipocyte differentiation. *J Biol Chem* 2004;279:52361–5.
72. Johnson SM, Grosshans H, Shingara J, et al. RAS is regulated by the let-7 microRNA family. *Cell* 2005;120:635–47.
73. Cheng J, Kapranov P, Drenkow J, et al. Transcriptional maps of 10 human chromosomes at 5-nucleotide resolution. *Science* 2005;308:1149–54.

Gene Expression Profiles in Peripheral Lymphocytes by Arsenic Exposure and Skin Lesion Status in a Bangladeshi Population

Maria Argos, Muhammad G. Kibriya, Faruque Parvez, et al.

Cancer Epidemiol Biomarkers Prev 2006;15:1367-1375.

Updated version Access the most recent version of this article at:
<http://cebp.aacrjournals.org/content/15/7/1367>

Cited articles This article cites 62 articles, 15 of which you can access for free at:
<http://cebp.aacrjournals.org/content/15/7/1367.full#ref-list-1>

Citing articles This article has been cited by 3 HighWire-hosted articles. Access the articles at:
<http://cebp.aacrjournals.org/content/15/7/1367.full#related-urls>

E-mail alerts [Sign up to receive free email-alerts](#) related to this article or journal.

Reprints and Subscriptions To order reprints of this article or to subscribe to the journal, contact the AACR Publications Department at pubs@aacr.org.

Permissions To request permission to re-use all or part of this article, use this link
<http://cebp.aacrjournals.org/content/15/7/1367>.
Click on "Request Permissions" which will take you to the Copyright Clearance Center's (CCC) Rightslink site.